# CONVECTIVE FLOW AND HEAT TRANSFER IN COMPOSITE FLUID AND POROUS LAYERS IN A ROTATING INCLINED MEDIUM

Karuna Sree Chitturi[1] , Sri Ramachandra Murty Paramsetti[2*] ,Sobhan Babu K[3], Archana Patil[4] , M.V.Ramana Murthy[5] , K L Vasundhara[6]

[1]Division of Mathematics, Vignan's Foundation for Science, Technology and Research, Vadlamudi, Andhra Pradesh, 522213 India. Mail id : [1]karuna637@gmail.com
[2*]Department of Mathematics, GSS, GITAM(Deemed to be University), Visakhapatnam, Andhra Pradesh, 530045 India. Mail id : [2*]dparamse@gitam.edu
[3]Department of Mathematics, University College of Engineering (Narasaraopet), Jawaharlal Nehru Technological University, Kakinada, Andhra Pradesh, 533003 India. Mail id :[3]ksobhanjntu@gmail.com
[4]Asst. Professor ,Dept. of Computer Science & Engineering, Rishi MS Institute of Engineering and Technology for women, Hyderabad, Telangana, India. Mail id : archanbpatil@gmail.com
[5]Former Professor And Chairman In Computer Science and Mathematics, Osmania university, 7556, Covington Pl, Rancho Cuca Monga, California, 91730, U S A .Mail id : ramanamurthymv09@gmail.com
[6]Dept of Mathematics, Stanly Engg College for Women, Abids, Hyderabad-1,India,

## Abstract

**The convective motion and heat variation between the two parallel inclined plates containing composite fluid and porous layers, in which the pressure gradient is kept constant, is analytically studied. The fluids in all the domains are distinct in thermal conductivities, viscosities and densities. The flow is believed to be continuous, laminar and completely formed. The governing equations are non-linear and coupled due to the inclusion of buoyancy forces, viscous and Darcy dissipation concepts. Solutions for region II are obtained by solving as ordinary differential equations and solutions are obtained using Perturbation Method for Region I and Region III. The effects of the governing parameters on the fluid flow are numerically computed and graphically depicted and inspected in detail. It is observed that with an increment in the value of porous parameter, both the axial and transverse velocities in all the regions decrease. Due to the Coriolis force axial velocity decreases with increasing rotation. Also it is noticed that the transverse velocity increases as the rotation parameter R increases.**

**Keywords:** **Convective flow, heat variation, inclined plates, porous layers, composite, fluid layer, rotation.**

## 1 INTRODUCTION

Due to its numerous practical uses in drying technology, energy storage systems and packed bed heat exchangers, nuclear waste respiratory and geothermal units convective heat transfer in a porous media has been the subject of numerous recent studies. One fluid occupying the entire closure case was studied in most of the existing research. The fluid system frequently consists two or more separate, immiscible fluid as well as sheets of one liquid over another, times in realistic situations. The behavior of a two fluid flow is of great importance when designing and conducting fluid experiments in low pull area. Even a multilayered fluid arrangement gives a modified model for growing high quality crystals which involve the buoyancy-driven convective process.

An understanding of the convective interaction of composite porous and fluid layers requires modeling of such systems. Fluid flow is also a normal phenomenon within a revolving structure. The velocity, density, volume, etc., will have an effect on the fluid particles internally and rises as the fluid

***Corresponding author.**

rotates. Fluid rotation can be limited, but cannot be disregarded. Flow in a revolving system has ample industrial and technical applications. Natural convection and fluid flow in an inclined and porous layer was analyzed by (Bian et al.[1], Kuznetsov et al.[2], Malashetty et al.[3-5], Komurgoz et al.[6], Simon and Shagaiya[7], Lima et al.[8] and Sri Ramachandra Murty et al.[9]). Flow and heat transfer in an inclined composite fluid and porous layers was investigated by Malashetty et al.[3] and couple stress composite viscous fluids were studied by Umavathi et al.[10]

Umavathi et al.[11] studied on the flow and heat transfer of composite micro polar and viscous fluids. Chauhan and Rastogi[12] analyzed the impact of heat transfer and hall current on MHD flow in a rotating system partially filled with porous layer.
Umavathi et al.[13] analyzed the unsteady flow and heat transfer of porous media sandwiched between viscous fluids. Sheikholeslami and Ganji[14] studied the impact of heat and mass transfer on nano fluid in a rotating system in three phase flow. Murty et al.[15] studied on the flow and heat transfer effects in an inclined rotating system of composite layers. Murty et al.[9] investigated on flow and heat transfer of MHD two fluid flow in an inclined channel. Recently Karuna et al. [16, 17] investigated convective flow and temperature distribution of porous medium in an inclined rotating system and convective flow and temperature distribution in rotating composite fluid layers. Rani et al.[18] investigated on convective properties of two fluids in a transverse magnetic field with in a inclined rotating channel and VeeraKumar et al.[19] studied unsteady rotating MHD flow of an infinite vertical moving porous surface. Even though the study on convective flow and temperature distribution through viscous fluid sandwiched between porous medium with inclined geometry is applied in many areas especially in geophysical systems, there appears to be a very limited number of researchers. The present work is focused on studying the impact of the parameters such as inclination angle, rotation and porous parameters, etc., on convective flow and heat transfer of MHD through an inclined rotating system of composite fluid layers.

## 2 MATERIALS AND METHODS

Physical representation of the present problem is laid - out in Figure 1. It is composed of two plates which are inclined, parallel and infinite in length along x and z-directions. The upper and and lower plate temperatures, $T_{w_1}$, $T_{w_1}$ and $T_{w_2}$ are kept stable. 'Φ' is the angle made by the inclined channel with the horizontal plane. The regions with $-h \le y \le 0$ and $h \le y \le 2h$ are loaded with two different homogeneous isotropic porous materials of permeability k, viscosity $\mu_1$, density $\rho_1$ and thermal conductivity $K_1$. The region $0 \le y \le h$ is filled with saturated viscous fluid of density $\rho_2$, viscosity $\mu_2$ and thermal conductivity $K_2$. Both the porous media are assumed to be homogeneous and isotropic. The three fluids have constant transport properties with laminar flow, fully developed and are assumed to be in a steady state. The flow in the channel is navigated by $\Delta T = T_{w_1} - T_{w_2}$ temperature gradient and pressure gradient $\left(\frac{-\partial p}{\partial x}\right)$ which is constant and is not influenced by heat transfer. The entire system is rotated with the angular velocity $\Omega$, about the y- axis.

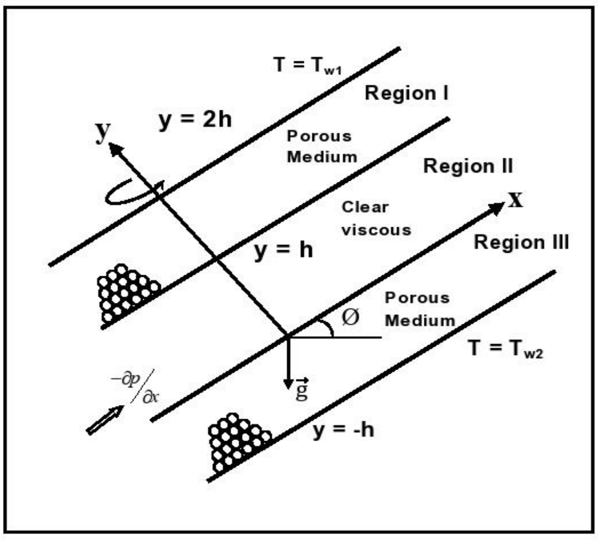


Figure1. Physical model

*Corresponding author.

Then the equations of motion and energy for Boussinesq fluids are:

**Region-I**

$$\mu_1 \frac{d^2 u_1}{dy^2} + \rho_1 g \beta_1 \sin\phi \left( T_1 - T_{w_2} \right) - \frac{\mu_1}{k} u_1 = \frac{\partial p}{\partial x} + 2\rho_1 \Omega w_1 \tag{1}$$

$$\mu_1 \frac{d^2 w_1}{dy^2} - \frac{\mu_1}{k} w_1 = -2\rho_1 \Omega u_1 \tag{2}$$

$$\frac{d^2 T_1}{dy^2} + \frac{\mu_1}{K_1 k} \left( u_1{}^2 + w_1{}^2 \right) = 0 \tag{3}$$

**Region-II**

$$\mu_2 \frac{d^2 u_2}{d\,y^2} + \rho_2 \, g \, \beta_2 \sin\phi \left( T_2 - T_{w_2} \right) = \frac{\partial p}{\partial x} + 2\rho_2 \Omega \, w_2 \tag{4}$$

$$\mu_2 \frac{d^2 w_2}{d\,y^2} = -2\rho_2 \Omega u_2 \tag{5}$$

$$K_2 \frac{d^2 T_2}{d\,y^2} = 0 \tag{6}$$

**Region-III**

$$\mu_1 \frac{d^2 u_3}{d\,y^2} + \rho_1 \, g \, \beta_1 \sin\phi \left( T_3 - T_{w_2} \right) - \frac{\mu_1}{k} u_3 = \frac{\partial p}{\partial x} + 2\rho_1 \Omega w_3 \tag{7}$$

$$\mu_1 \frac{d^2 w_3}{d\,y^2} - \frac{\mu_1}{k} w_3 = -2\rho_1 \Omega \, u_3 \tag{8}$$

$$\frac{d^2 T_3}{d\,y^2} + \frac{\mu_1}{K_1 k} \left( u_3{}^2 + w_3{}^2 \right) = 0 \tag{9}$$

where $u_i$ and $w_i$ are the x-component and z-component of fluid velocity, where subscript, $i = 1, 2, 3$ represents values for phases I, II, III. The thermal expansion coefficient is $\beta_i$ and of temperature is $T_i$. Due to the no-slip condition, the velocity must be vanishing at the wall. The respective boundary and interface conditions with the above conditions on velocity and temperature distributions are:

*Corresponding author.

$$u_1(2h)=0,\ \ w_1(2h)=0;\ \ u_1(h)=u_2(h),$$
$$w_1(h)=w_2(h);\ u_2(0)=u_3(0),$$
$$w_2(0)=w_3(0)\ \ u_3(-h)=0,\ \ w_3(-h)=0$$
$$\mu_1\frac{du_1}{dy}=\mu_2\frac{du_2}{dy}\quad and$$
$$\mu_1\frac{dw_1}{dy}=\mu_2\frac{dw_2}{dy}\quad when\ \ y=h$$
$$\mu_2\frac{du_2}{dy}=\mu_1\frac{du_3}{dy}\quad at\ \ y=0\ \ and$$
$$\mu_2\frac{dw_2}{dy}=\mu_1\frac{dw_3}{dy}\quad when\ \ y=0 \qquad (10)$$

$$T_2(0)=T_3(0), T_1(2h)=T_{w_1},$$
$$T_1(h)=T_2(h), T_3(-h)=T_{w_2}$$
$$K_1\frac{dT_1}{dy}=K_2\frac{dT_2}{dy}\ when\ y=h$$
$$and\ K_2\frac{dT_2}{dy}=K_1\frac{dT_3}{dy}\ when\ y=0 \qquad (11)$$

To make these equations dimensionless, the transformations used are:

$$\frac{u_1}{\bar{u}_1}=u_1^*,\quad \frac{u_2}{\bar{u}_1}=u_2^*,\quad \frac{u_3}{\bar{u}_1}=u_3^*,\quad \frac{w_1}{\bar{u}_1}=w_1^*,\quad \frac{w_2}{\bar{u}_1}=w_2^*,\quad \frac{w_3}{\bar{u}_1}=w_3^*,$$
$$\Pr=\frac{\mu_1 C_p}{K_1},\ \lambda=\frac{h}{\sqrt{k}},\ \ \mathrm{Re}=\frac{\bar{u}_1 h}{\nu_1},\ K=\frac{K_1}{K_2},\ \ n=\frac{\rho_1}{\rho_2},$$
$$b=\frac{\beta_1}{\beta_2},\quad R^2=\frac{\Omega h^2}{\nu_1}$$
$$Ec=\frac{\bar{u}_1^{\,2}}{C_p(T_{w1}-T_{w2})},\quad \left[\frac{(T-T_{w2})}{(T_{w1}-T_{w2})}\right]=\theta,$$
$$Gr=\frac{g\beta_1 h^3(T_{w1}-T_{w2})}{\nu_1^2},\quad P=\left(\frac{h^2}{\mu_1\bar{u}_1}\right)\left(\frac{\partial p}{\partial x}\right).$$

Here average velocity is indicated by $\bar{u}_1$.
Applying the above transformations, the Equations (1)-(9) transform to:

**Region-I**

*Corresponding author.

$$\frac{d^2u_1}{dy^2}+\frac{Gr}{Re}(Sin\phi)\theta_1-\lambda^2u_1=P+2R^2w_1 \tag{13}$$

$$\frac{d^2w_1}{dy^2}-\lambda^2w_1=-2R^2u_1 \tag{14}$$

$$\frac{d^2\theta_1}{dy^2}+\Pr Ec\ \lambda^2(u_1{}^2+w_1{}^2)=0 \tag{15}$$

**Region-II**

$$\frac{d^2u_2}{dy^2}+\frac{mGr}{nb\,\mathrm{Re}}(Sin\phi)\theta_2=mP+2R^2w_2 \tag{16}$$

$$\frac{d^2w_2}{dy^2}=-2R^2u_2 \tag{17}$$

$$\frac{d^2\theta_2}{dy^2}=0 \tag{18}$$

**Region-III**

$$\frac{d^2u_3}{dy^2}+\frac{Gr}{Re}(Sin\phi)\theta_3-\lambda^2u_3=P+2R^2w_3 \tag{19}$$

$$\frac{d^2w_3}{dy^2}-\lambda^2w_3=-2R^2u_3 \tag{20}$$

$$\frac{d^2\theta_3}{dy^2}+\Pr Ec\ \lambda^2(u_3{}^2+w_3{}^2)=0 \tag{21}$$

$$\begin{gathered}\theta_1(1+h)=1,\ \ \theta_1(h)=\theta_2(h),\\ \theta_2(0)=\theta_3(0),\theta_3(-1)=0,\\ K\frac{d\theta_1}{dy}=\frac{d\theta_2}{dy}\ \ when\ y=h\ ,\\ \frac{1}{K}\frac{d\theta_2}{dy}=\frac{d\theta_3}{dy}\ \ when\ \ y=0.\end{gathered} \tag{22}$$

Considering $q_{1i}=u_{1i}+i\,\omega_{1i}$, $q_2=u_2+i\,\omega_2$
for i = 0, 1 and $q_{3i}=u_{3i}+i\,\omega_{3i}$,

Equations (13)-(21) in complex form are:

*Corresponding author.

**Region-*I***

$$\frac{d^2q_1}{dy^2}+\frac{Gr}{Re}(Sin\ \phi)\theta_1-\lambda^2q_1=P-2iR^2q_1 \qquad (23)$$

$$\frac{d^2\theta_1}{dy^2}+\Pr Ec\lambda^2(q_1\overline{q_1})=0 \qquad (24)$$

**Region-II**

$$\frac{d^2q_2}{d\,y^2}+\frac{mGr}{nb\,\mathrm{Re}}(Sin\ \phi)\theta_2=mP-2iR^2q_2 \qquad (25)$$

$$\frac{d^2\theta_2}{d\,y^2}=0 \qquad (26)$$

**Region-III**

$$\frac{d^2q_3}{d\,y^2}+\frac{Gr}{Re}(Sin\ \phi)\theta_3-\lambda^2q_3=P-2iR^2q_3 \qquad (27)$$

$$\frac{d^2\theta_3}{d\,y^2}+\Pr Ec\lambda^2(q_3\overline{q_3})=0 \qquad (28)$$

The dimensionless forms of the interface and boundary conditions are:

$u_1(h+1)=0,\ w_1(h+1)=0,\ \ u_1(h)=u_2(h),\ w_1(h)=w_2(h),\ \ u_2(0)=u_3(0),$
$w_2(0)=w_3(0),\ u_3(-1)=0,\ \ w_3(-1)=0,$
$\frac{du_1}{dy}=\frac{1}{m}\frac{du_2}{dy}$ and $\frac{dw_1}{dy}=\frac{1}{m}\frac{dw_2}{dy}$
when y = h,

$\frac{du_2}{dy}=m\frac{du_3}{dy}$ and $\frac{dw_2}{dy}=m\frac{dw_3}{dy}$ when y =0
$\bar{q}_1$ , $\bar{q}_3$ are the complex conjugate of $q_1\ and\ q_3$

The respective boundary and interface conditions are:

$$q_1(2)=0,\ q_2(0)=q_3(0),$$
$$q_1(1)=q_2(1),\ \ q_3(-1)=0,$$
$$\frac{dq_1}{dy}=\frac{1}{m}\frac{dq_2}{dy} \quad when\ \ y=1,$$
$$\frac{dq_2}{dy}=m\frac{dq_3}{dy} \quad when\ y=0 \qquad (29)$$

*Corresponding author.

$$\theta_1(2)=1,\ \theta_1(1)=\theta_2(1),$$
$$\theta_2(0)=\theta_3(0), \theta_3(-1)=0,$$
$$K\frac{d\theta_1}{dy}=\frac{d\theta_2}{dy}\quad when\ y=1\ ,$$
$$\frac{1}{K}\frac{d\theta_2}{dy}=\frac{d\theta_3}{dy}\quad when\ y=0. \qquad (30)$$

## 2.1 SOLUTIONS OF THE PROBLEM

Hence the closed form solutions are obtained using the method of ordinary differential equations as the governing energy and momentum equations for Region II are linear ordinary differential equations. The equations for Region II are:

**Region II**

$$\frac{d^2q_2}{dy^2}+\frac{mGr}{nb\mathrm{Re}}(\sin\varphi)\theta_2=mP-2iR^2q_2 \qquad (31)$$

$$\frac{d^2\theta_2}{dy^2}=0 \qquad (32)$$

For Region I and Region III the governing momentum and energy equations are non-linear and coupled. Hence to obtain approximate solutions we used Perturbation Method. Pr.Ec (=ε), the perturbation parameter, which is small, is used as the perturbation quantity. The solutions for Region I and III are considered as

$$(q_i,\theta_i)=(q_{i0},\theta_{i0})+\varepsilon(q_{i1},\theta_{i1})+\ldots\ldots \qquad (33)$$

Where $q_{i0},\theta_{i0}$ are solutions of zeroth-order, for the case when ε is equal to zero and $q_{i1},\theta_{i1}$ are quantities perturbed related to $q_{i0},\theta_{i0}$ respectively. Using the above in Equations (23), (24), (27) and (28) and equating the respective coefficients of existing identical powers of ε, we obtain equations of zeroth-order and First-order approximations for Region-I and Region III are as follows:

**Region-I**

Equations of zero$^{th}$-order approximation

$$\frac{d^2q_{10}}{dy^2}+\frac{Gr}{\mathrm{Re}}(\sin\varphi)\theta_{10}-\lambda^2q_{10}=P-2iR^2q_{10} \qquad (34)$$

$$\frac{d^2\theta_{10}}{dy^2}=0 \qquad (35)$$

Equations of first-order approximation

$$\frac{d^2q_{11}}{dy^2}+\frac{Gr}{\mathrm{Re}}(\sin\varphi)\theta_{11}-\lambda^2q_{11}=-2iR^2q_{11}, \qquad (36)$$

$$\frac{d^2\theta_{11}}{dy^2}+\lambda^2(q_{10}\,\overline{q_{10}})=0 \qquad (37)$$

*Corresponding author.

**Region-III**

Equations of zero$^{th}$-order approximation

$$\frac{d^2 q_{30}}{dy^2} + \frac{Gr}{\mathrm{Re}}(\sin\varphi)\theta_{30} - \lambda^2 q_{30} = P - 2iR^2 q_{30} \tag{38}$$

$$\frac{d^2\theta_{30}}{dy^2} = 0 \tag{39}$$

Equations of first-order approximation

$$\frac{d^2 q_{31}}{dy^2} + \frac{Gr}{\mathrm{Re}}(\sin\varphi)\theta_{30} - \lambda^2 q_{31} = -2iR^2 q_{31}, \tag{40}$$

$$\frac{d^2\theta_{31}}{dy^2} + \lambda^2 (q_{30}\,\overline{q_{30}}) = 0 \tag{41}$$

**Boundary Conditions**

Zeroth Order

$$q_{10}(2) = 0, q_{10}(1) = q_2(1), q_2(0) = q_{30}(0),$$
$$q_{30}(-1) = 0, \frac{dq_{10}}{dy} = \frac{1}{m}\frac{dq_2}{dy} \quad when\ \ y = 1,$$
$$\frac{dq_2}{dy} = m\frac{dq_{30}}{dy}\ \ when\ \ y = 0, \tag{42}$$
$$\theta_{10}(2) = 1,\ \ \theta_{10}(1) = \theta_2(1),$$
$$\theta_2(0) = \theta_{30}(0),\ \theta_{30}(-1) = 0,$$
$$K\frac{d\theta_{10}}{dy} = \frac{d\theta_2}{dy}\ \ when\ \ y = 1\ ,$$
$$\frac{1}{K}\frac{d\theta_2}{dy} = \frac{d\theta_{30}}{dy}\ \ when\ \ y = 0. \tag{43}$$

First Order

$$q_{11}(2) = 0, q_{11}(1) = 0, q_{31}(0) = 0,\ q_{31}(-1) = 0$$
$$\text{when } y = 1, \frac{dq_{11}}{dy} = 0 \text{ and when } y = 0, \frac{dq_{31}}{dy} = 0 \tag{44}$$

It is noted that

$$q_{10} = u_{10} + iw_{10}, q_2 = u_2 + iw_2,$$
$$q_{11} = u_{11} + iw_{11}$$
$$q_{30} = u_{30} + iw_{30}, q_{31} = u_{31} + iw_{31} \tag{46}$$

Solutions of Equations (31), (32) and Equations (34)-(41) using boundary conditions (42) to (45) are:

*Corresponding author.

$$\theta_{10} = \frac{K+y}{2+K} \tag{47}$$

$$\theta_{2} = \frac{(1+Ky)}{2+K} \tag{48}$$

$$\theta_{30} = \frac{(1+y)}{2+K} \tag{49}$$

$$u_{10}=(b_1e^{Z_1y}+b_2e^{-Z_1y})\cos(Z_2y)+(t_7+t_9y) \tag{50}$$

$$w_{10}=-((b_1e^{Z_1y}-b_2e^{-Z_1y})\sin(Z_2y)-(t_8+t_{10}y)) \tag{51}$$

$$u_2=(b_7e^{-Ry}+b_8e^{Ry})\cos(Ry) \tag{52}$$

$$w_2=((b_7e^{-Ry}-b_8e^{Ry})\sin(Ry)+(t_1+t_2y)) \tag{53}$$

$$u_{30}=(b_9e^{Z_1y}+b_{10}e^{-Z_1y})\cos(Z_2y)+(t_{12}+t_{14}y) \tag{54}$$

$$w_{30}=-((b_9e^{Z_1y}-b_{10}e^{-Z_1y})\sin(Z_2y)-(t_{13}+t_{10}y)) \tag{55}$$

$$\begin{aligned}
\theta_{11}=\;& b_3+b_4y+L_{30}e^{2Z_1y}+L_{31}e^{-2Z_1y}+L_{32}\cos(2Z_2y)\\
&+L_{33}e^{Z_1y}y\sin(Z_2y)+L_{34}e^{Z_1y}\sin(Z_2y)+L_{35}e^{Z_1y}y\cos(Z_2y)\\
&+L_{36}e^{Z_1y}\cos(Z_2y)+L_{37}e^{-Z_1y}y\sin(Z_2y)+L_{38}e^{-Z_1y}\sin(Z_2y)\\
&+L_{39}e^{-Z_1y}y\cos(Z_2y)+L_{40}e^{-Z_1y}\cos(Z_2y)+L_{41}y^4+L_{42}y^3+L_{43}y^2\\
&+i(L_{44}\sin(2Z_2y)+L_{45}e^{Z_1y}y\sin(Z_2y)+L_{46}e^{Z_1y}\sin(Z_2y)\\
&+L_{47}e^{Z_1y}y\cos(Z_2y)+L_{48}e^{Z_1y}\cos(Z_2y)+L_{49}e^{-Z_1y}y\sin(Z_2y)\\
&+L_{50}e^{-Z_1y}\sin(Z_2y)+L_{51}e^{-Z_1y}y\cos(Z_2y)+L_{52}e^{-Z_1y}\cos(Z_2y))
\end{aligned} \tag{56}$$

***Corresponding author.**

$$\theta_{31}=b_{11}+b_{12}y+I_{30}e^{2Z_1y}+I_{31}e^{-2Z_1y}+I_{32}\cos(2Z_2y)$$
$$+I_{33}e^{Z_1y}y\sin(Z_2y)+I_{34}e^{Z_1y}\sin(Z_2y)+I_{35}e^{Z_1y}y\cos(Z_2y)$$
$$+I_{36}e^{Z_1y}\cos(Z_2y)+I_{37}e^{-Z_1y}y\sin(Z_2y)+I_{38}e^{-Z_1y}\sin(Z_2y)$$
$$+I_{39}e^{-Z_1y}y\cos(Z_2y)+I_{40}e^{-Z_1y}\cos(Z_2y)$$
$$+I_{41}y^4+I_{42}y^3+I_{43}y^2$$
$$+i(I_{44}\sin(2Z_2y)+I_{45}e^{Z_1y}y\sin(Z_2y)+I_{46}e^{Z_1y}\sin(Z_2y)$$
$$+I_{47}e^{Z_1y}y\cos(Z_2y)+I_{48}e^{Z_1y}\cos(Z_2y)+$$
$$I_{49}e^{-Z_1y}y\sin(Z_2y)+I_{50}e^{-Z_1y}\sin(Z_2y)$$
$$+I_{51}e^{-Z_1y}y\cos(Z_2y)+I_{52}e^{-Z_1y}\cos(Z_2y)) \qquad (57)$$

$$u_{11}= (b_5e^{Z_1y}+b_6e^{-Z_1y})\cos(Z_2y)+N_{75}+N_{76}y$$
$$+N_{77}y^2+N_{13}y^3+N_{17}y^4+N_{23}\cos(2Z_2y)$$
$$-N_{50}\sin(2Z_2y)+N_{78}e^{Z_1y}\cos(Z_2y)+N_{79}e^{Z_1y}\sin(Z_2y)$$
$$+N_{80}e^{-Z_1y}\cos(Z_2y)+N_{81}e^{-Z_1y}\sin(Z_2y)$$
$$+N_{41}e^{Z_1y}y\cos(Z_2y)-N_{32}e^{Z_1y}y\sin(Z_2y)$$
$$-N_5e^{2Z_1y}-N_7e^{-2Z_1y}+N_{82}e^{-Z_1y}y\cos(Z_2y)$$
$$+N_{83}e^{-Z_1y}y\sin(Z_2y)+N_{84}y^2e^{-Z_1y}\cos(Z_2y)$$
$$+N_{85}y^2e^{-Z_1y}\sin(Z_2y)) \qquad (58)$$

*Corresponding author.

$$
\begin{aligned}
w_{11} = {} & (b_6 e^{-Z_1 y} - b_5 e^{Z_1 y})\sin(Z_2 y) + N_{86} + N_{87} y \\
& + N_{88} y^2 + N_{14} y^3 + N_{18} y^4 + N_{24}\cos(2Z_2 y) \\
& + N_{49}\sin(2Z_2 y) + N_{89} e^{Z_1 y}\cos(Z_2 y) \\
& + N_{90}{}^{Z_1 y}\sin(Z_2 y) + N_{91} e^{-Z_1 y}\cos(Z_2 y) \\
& + N_{92} e^{-Z_1 y}\sin(Z_2 y) + N_{61} e^{Z_1 y} y\cos(Z_2 y) \\
& - N_{58} e^{Z_1 y} y\sin(Z_2 y) + N_6 e^{2Z_1 y} \\
& + N_8 e^{-2Z_1 y} + N_{93} e^{-Z_1 y} y\cos(Z_2 y) \\
& + N_{94} e^{-Z_1 y} y\sin(Z_2 y) + N_{95} y^2 e^{-Z_1 y}\cos(Z_2 y) \\
& + N_{96} y^2 e^{-Z_1 y}\sin(Z_2 y) \qquad (59)
\end{aligned}
$$

$$
\begin{aligned}
u_{31} = {} & (b_{13} e^{Z_1 y} + b_{14} e^{-Z_1 y})\cos(Z_2 y) + M_{75} + M_{76} y \\
& + M_{77} y^2 + M_{13} y^3 + M_{17} y^4 + M_{23}\cos(2Z_2 y) \\
& - M_{50}\sin(2Z_2 y) + M_{78} e^{Z_1 y}\cos(Z_2 y) \\
& + M_{79} e^{Z_1 y}\sin(Z_2 y) + M_{80} e^{-Z_1 y}\cos(Z_2 y) \\
& + M_{81} e^{-Z_1 y}\sin(Z_2 y) + M_{41} e^{Z_1 y} y\cos(Z_2 y) \\
& - M_{32} e^{Z_1 y} y\sin(Z_2 y) - M_5 e^{2Z_1 y} - M_7 e^{-2Z_1 y} \\
& + M_{82} e^{-Z_1 y} y\cos(Z_2 y) + M_{83} e^{-Z_1 y} y\sin(Z_2 y) \\
& + M_{84} y^2 e^{-Z_1 y}\cos(Z_2 y) + M_{85} y^2 e^{-Z_1 y}\sin(Z_2 y)) \qquad (60)
\end{aligned}
$$

$$
\begin{aligned}
w_{31} = {} & (b_{14} e^{-Z_1 y} - b_{13} e^{Z_1 y})\sin(Z_2 y) + M_{86} + M_{87} y \\
& + M_{88} y^2 + M_{14} y^3 + M_{18} y^4 + M_{24}\cos(2Z_2 y) \\
& + M_{49}\sin(2Z_2 y) + M_{89} e^{Z_1 y}\cos(Z_2 y) + M_{90}{}^{Z_1 y}\sin(Z_2 y) \\
& + M_{91} e^{-Z_1 y}\cos(Z_2 y) + M_{92} e^{-Z_1 y}\sin(Z_2 y) \\
& + M_{61} e^{Z_1 y} y\cos(Z_2 y) - M_{58} e^{Z_1 y} y\sin(Z_2 y) \\
& + M_6 e^{2Z_1 y} + M_8 e^{-2Z_1 y} + M_{93} e^{-Z_1 y} y\cos(Z_2 y) \\
& + M_{94} e^{-Z_1 y} y\sin(Z_2 y) + M_{95} y^2 e^{-Z_1 y}\cos(Z_2 y) \\
& + M_{96} y^2 e^{-Z_1 y}\sin(Z_2 y) \qquad (61)
\end{aligned}
$$

* **Corresponding author.**

Equations (50)-(61) are numerically solved by using the parameter frame as (n, Re, b, P) = (1.5, 5, 1 - 5) and the constants involved in them are not given because of shortness. In the Figures 2 and 3, all other values are taken from the set ($\lambda$, R, Gr,$\phi$, m, K) = ( 2,1,5,30°, 0.5, 1), excluding the varying one.

## 3 RESULTS AND DISCUSSIONS

Three layered fluid, in an inclined channel of fluid sandwiched between two porous layers and heat transfer outcomes are studied. The influence of porous parameter $\lambda$ on velocity field is shown in Figure 2(a) and Figure 2(b). With an increment in the value of $\lambda$ both the axial and transverse velocities in all the regions decrease. The velocity fields for Region I and Region III, which consist of porous fluids, are large compared to the region II, which consists of clear fluid. The clear fluid in region II drags the fluid back on either side of the porous layer. Furthermore it is important to note that the maximum velocity occurs at the centre of the region II. It is also found that the presence of two porous layers on either side of the fluid layer decreases the mass flow rate in the fluid medium. This indicates that the porous matrix has a significant influence on the field of velocity.

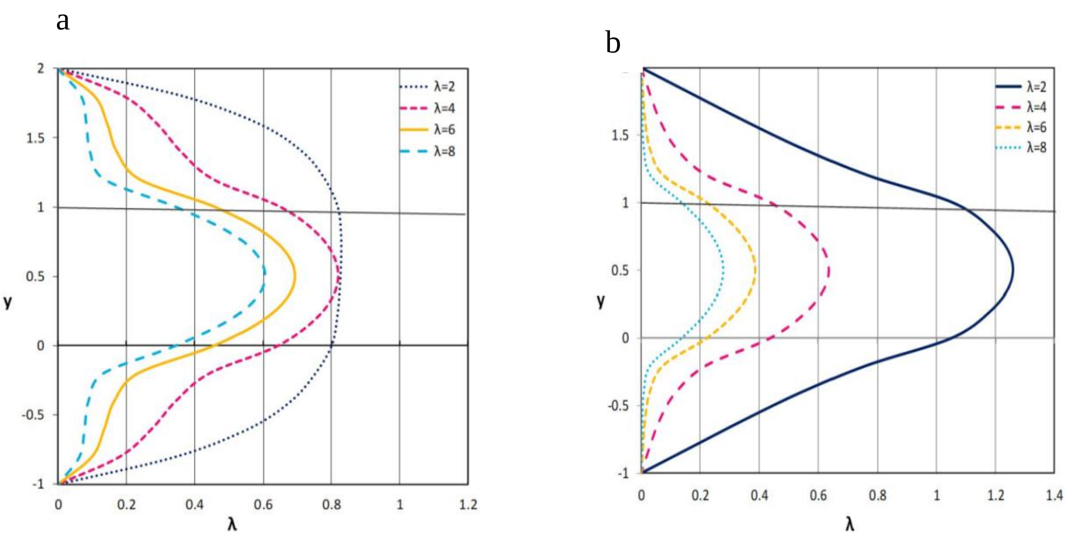


**FIGURE 2** Velocity distribution of $\lambda$ (a) Axial (b) Transverse

The outcome of m, the ratio of viscosities is shown in Figure 3(a) and Figure 3(b). Increment in the values of m indicates the increase in both axial and transverse velocities.

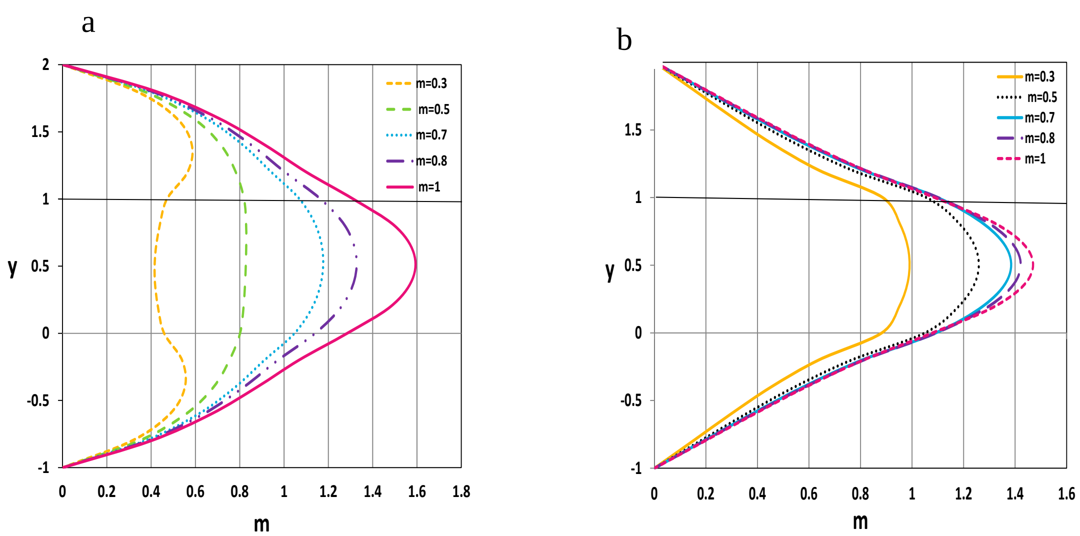


**FIGURE 3** Velocity distribution of m (a) Axial (b) Transverse

*Corresponding author.

The effect of Gr, the Grashof number, depicted in Figure 4 (a) and Figure 4 (b) shows that both velocities increase as Gr value increases.

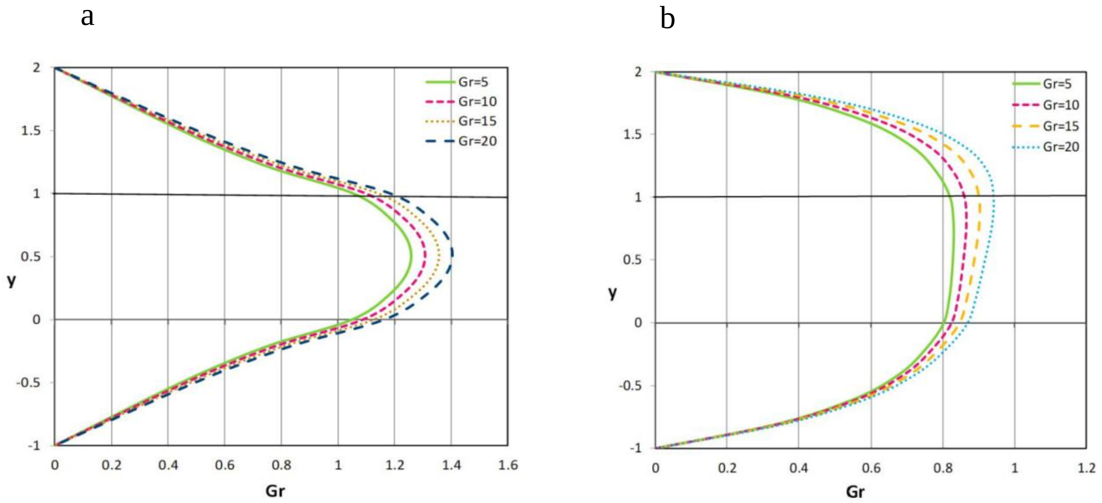


**FIGURE 4** Velocity distribution of Gr (a) Axial (b) Transverse

The effect of ϕ the inclination angle is shown in Figure 5 (a) and Figure 5 (b), indicating that as the value of ϕ increases both the axial and transverse velocities increase.

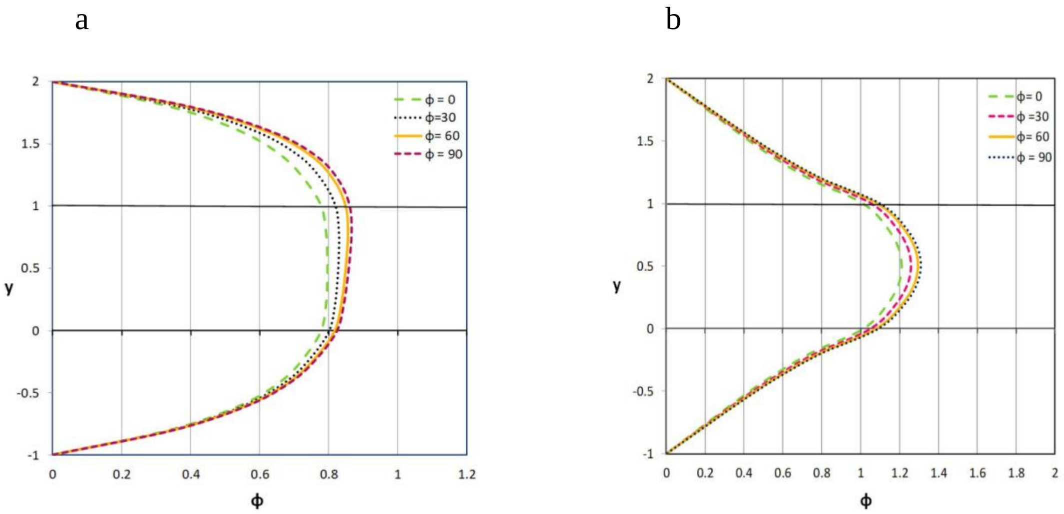


**FIGURE 5** Velocity distribution of ϕ (a) Axial (b) Transverse

The effect of R, the rotation parameter on velocity field is shown in Figure 6(a) and Figure 6(b). It is noticed that because of the Coriolis force axial velocity reduces with increasing rotation. Also it is noticed that the transverse velocity increases as the rotation parameter R increases in (0, 0.7), but outside the range as R increases it decreases. Further it is noticed that for all the parameters the graphs are symmetric in region I and III, velocity in the fluid region is more when compared with porous layers.

*Corresponding author.

a

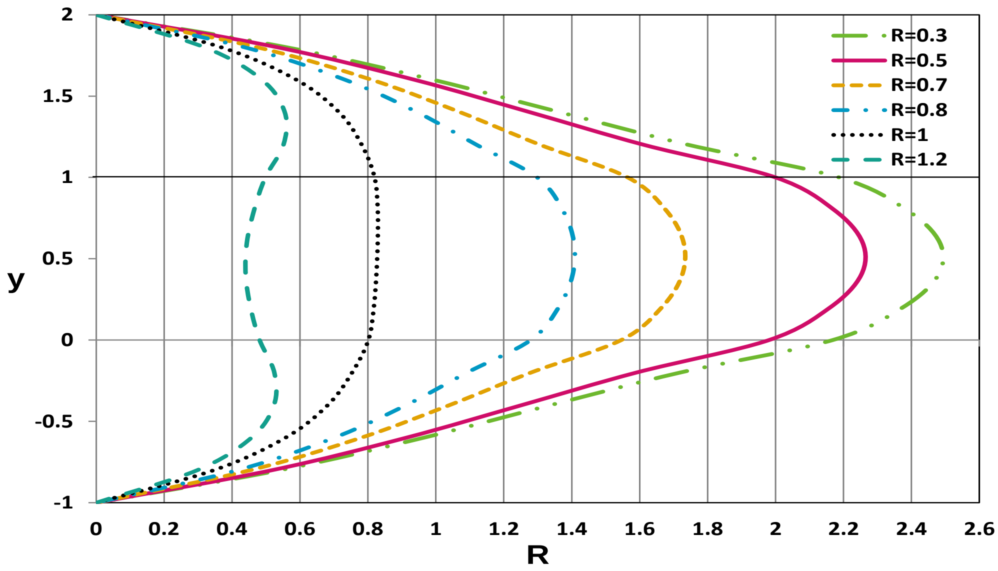


b

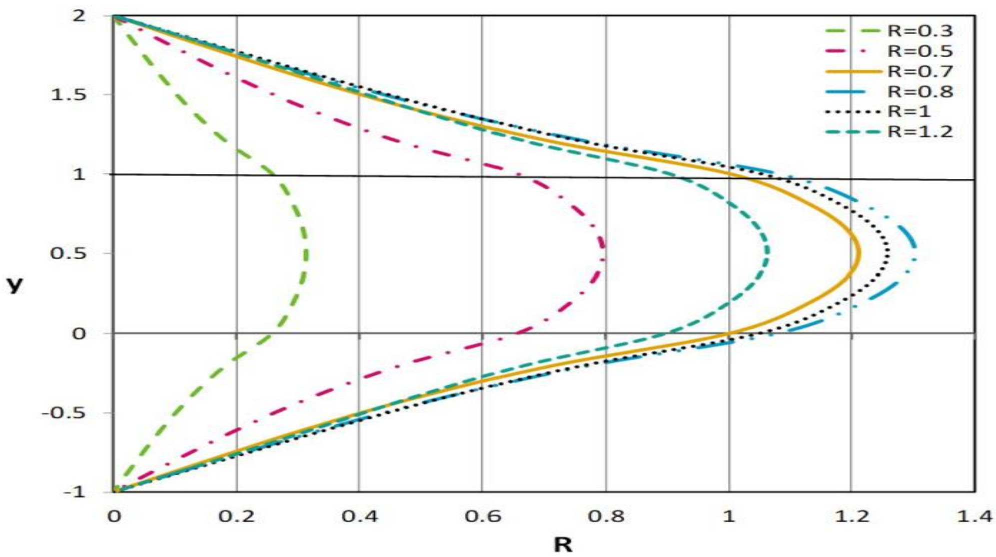


**FIGURE 6** Velocity distribution of (a) Axial (b) Transverse

The effect on the temperature field by the physical parameters is shown in Figure 7(a) to Figure 7(e). Temperature profiles for region I and III are non-linear and linear for region II for all the governing parameters. Figure 7(a) displays the effect of porous parameter $\lambda$ on temperature. The increasing values of $\lambda$ decreases the temperature in Region I and III. The effect of ratio of viscosities m is shown in Figure 7 (b). Increment in the values of m indicates the rise in temperature in region I and III. Figure 7 (c) indicates the effect of Grashof number Gr, showing that as the value of Gr increases the temperature increases in Region I and III.

The outcome on the temperature by the angle of inclination $\phi$ is shown in Figure 7 (d), indicating that in Region I and III as the value of $\phi$ increases temperature increases. The effect of rotation parameter R is shown in Figure 7 (e), which conveys that the temperature decreases in Region I and III as the value of R increases.

*Corresponding author.

a

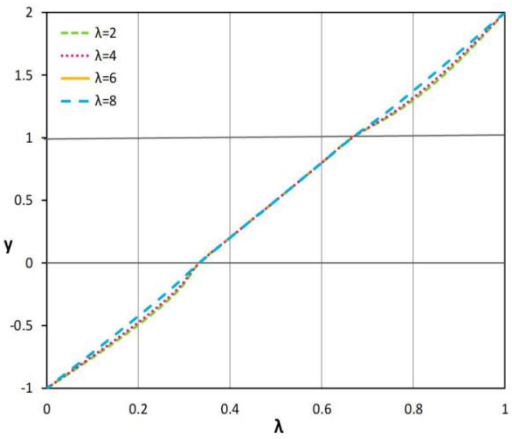


b

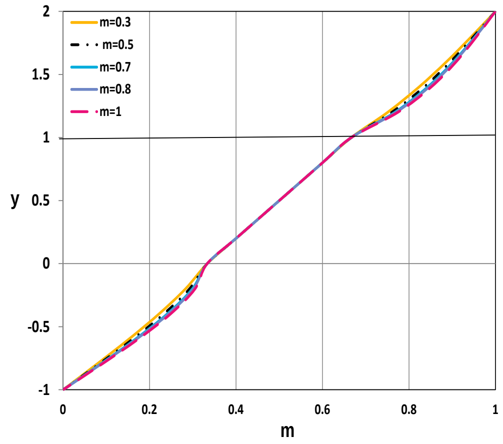


c

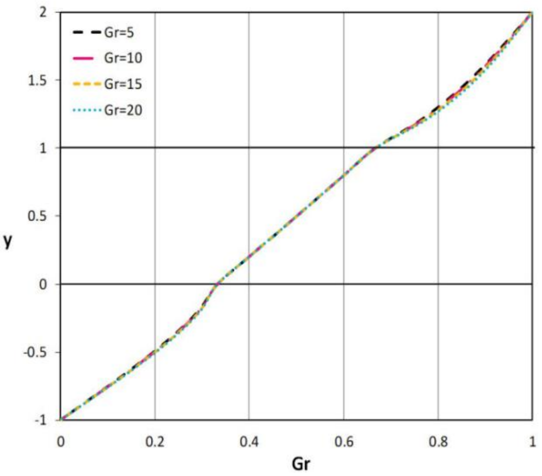


d

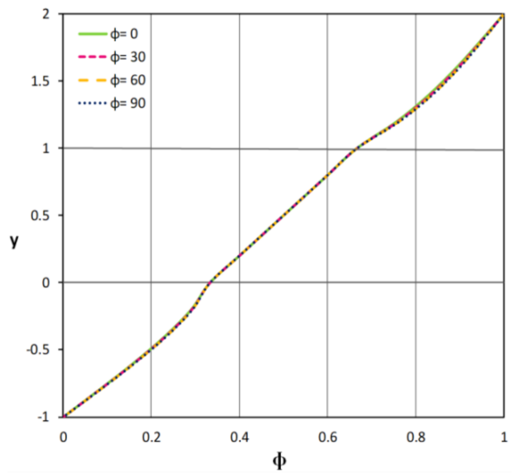


e

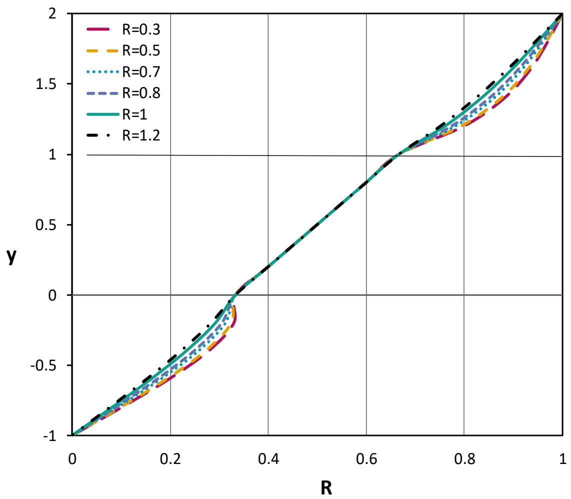


*Corresponding author.

**FIGURE 7** Temperature distribution (a) λ (b) m (c) Gr (d) ϕ (e) R

In addition to analyze temperature distribution and impact of velocity on fluid flow it is also important to observe the effect of physical properties such as Skin Friction and Nusselt number.

The Skin Friction at the upper plate is given by $\left(\frac{du_1}{dy}\right)_{y=2} = \tau_T$ and

The Skin Friction at the lower plate is given by $\left(\frac{du_3}{dy}\right)_{y=-1} = \tau_B$ .

Similarly the rate of heat transfer from the wall to the fluid, knowing the temperature distribution, at the upper plate ($q_T$) and lower plate ($q_B$) is given by

$\left(\frac{d\Theta_1}{dy}\right)_{y=2} = q_T$ , $\left(\frac{d\Theta_3}{dy}\right)_{y=-1} = q_B$

The numerical values of Skin-friction and Nusselt number are given in Table 1 It is noted that the rate of heat transfer is invariable for upper and lower plates. As the values of parameter λ increases, the skin friction increases for upper plate and decreases for lower plate. As the value of R increases, the skin friction for the upper and lower plate increases and then decreases. For the parameters Gr, ϕ, m and h as the values increase the skin friction decreases at both plates. As the value of λ and R increases, the rate heat transfer also increases, but decreases for Gr, ϕ, and m. At the lower plate no heat transfer is observed.

**TABLE1**: **Skin friction and Nusselt number at both upper and lower plates with different physical parameters.**

| Physical Parameter | Skin friction at the upper plate ($\tau_T$) | Skin friction at the lower plate ($\tau_B$) | Nusselt number at the upper plate ($q_T$) | Nusselt number at the lower plate ($q_B$) |
|---|---|---|---|---|
| λ = 2 | -0.6136 | 1.62637 | 0.252076 | 0 |
| λ = 4 | -1.0314 | 1.25782 | 0.268208 | 0 |
| λ = 6 | -0.8064 | 0.81386 | 0.296677 | 0 |
| λ = 8 | -0.6412 | 0.61650 | 0.311166 | 0 |
| R=0.1 | -4.8933 | 3.71492 | 0.146935 | 0 |
| R=0.3 | -4.8073 | 3.66720 | 0.149231 | 0 |
| R=0.5 | -3.4173 | 1.65452 | 0.163287 | 0 |
| R=0.7 | -2.9746 | 2.67050 | 0.195942 | 0 |
| R = 1 | -0.6136 | 1.62637 | 0.252076 | 0 |
| R=1.2 | -0.1328 | 0.44384 | 0.276596 | 0 |
| R = 1.5 | -1.2865 | -0.0026 | 0.259692 | 0 |
| R = 2 | -0.7690 | 0.71080 | 0.311083 | 0 |
| R = 3 | -1.1426 | 0.7489 | 0.314799 | 0 |
| R = 4 | -0.3297 | -0.0953 | 0.32558 | 0 |
| Gr =5 | -0.6136 | 1.6264 | 0.25208 | 0 |
| Gr =10 | -0.8305 | 0.8309 | 0.24192 | 0 |
| Gr =15 | -1.0800 | 0.37227 | 0.231134 | 0 |
| Gr =20 | -1.3633 | -0.1120 | 0.219733 | 0 |
| ϕ = 0 | -0.4278 | 1.6693 | 0.26162 | 0 |
| ϕ = 30 | -0.6136 | 1.62637 | 0.252076 | 0 |
| ϕ = 60 | -0.7693 | 0.95784 | 0.244698 | 0 |
| ϕ = 90 | -0.8305 | 0.83092 | 0.241915 | 0 |
| m = 0.5 | -0.6136 | 1.62637 | 0.252076 | 0 |
| m =1 | -0.7618 | 1.45311 | 0.216511 | 0 |

*Corresponding author.

| | | | | |
|---|---|---|---|---|
| m = 1.5 | -0.8340 | 1.54673 | 0.200450 | 0 |
| m = 2 | -0.5454 | 1.40972 | 0.191819 | 0 |

## 4 CONCLUSIONS

It is observed that the impact of the porous parameter is to retard the temperature, axial velocity and transverse velocity in three regions. The increase in buoyancy force incorporated through Grashof number and the angle of inclination is to enhance the temperature, axial and transverse velocities for the three layers. The decrease in the temperature and axial velocity of the fluid in the three regions is admitted by an increase in Coriolis force built into the rotation parameter. The flow and thermal aspects of the fluids in the channel are enhanced by an increase in the ratio of viscosities of the fluids of the three regions. In packed bed heat exchangers, drying technology, energy storage units, nuclear waste respiratory and geothermal systems the results of the three-layered flow and temperature distribution through an inclined fluid layer sandwiched between porous media could be useful.

## CONFLICT OF INTEREST

The authors declare that there are no conflict of interests.

**ORCID ID:** https://orcid.org/0000-0002-2355-8192

## REFERENCES

1. Bian, W., Vasseur, P., Bilgen, E., and Meng, F. (1996).Effect of an electromagnetic field on natural convection in an inclined porous layer. International Journal of Heat and Fluid Flow, 17:1, 36-44.
2. Kuznetsov, A.V. (1998). Analytical investigation of Couette flow in a composite channel partially filled with a porous medium and partially with a clear fluid. International Journal of Heat and Mass Transfer. 41:16, 2556-2560.
3. Malashetty, M.S., Umavathi, J.C., and Kumar, J.P. (2001). Convective flow and heat transfer in an inclined composite porous medium. Journal of Porous Medium. 4: 15-22.
4. Malashetty, M.S., Umavathi, J.C., and Pratapkumar, J. (2004). Two fluid flow and heat transfer in an inclined channel containing porous and fluid layer. Heat and Mass Transfer. 40:11,871-876.
5. Malashetty, M.S., Umavathi, J.C., Pratapkumar, J. (2005). Flow and heat transfer in an inclined channel containing a fluid layer sandwiched between two porous layers. Journal of Porous Media. 8:5, 443-453.
6. Komurgoz, G., Arikoglu, A., Turker, E., and Ibrahim O. (2010). Second-law analysis for an inclined channel containing porous-clear fluid layers by using the differential transform method. An International Journal of Computation and Methodology, Numerical Heat Transfer, Part A: Applications. 57: 603-623.
7. Simon, D., and Shagaiya Daniel, Y. (2013). Convective flow of two immiscible fluids and heat transfer with porous along an inclined channel with pressure gradient. Research Inventy: International Journal of Engineering and Science. 2(4): 12-18.
8. Lima, J.A., Assad, G.E., and Paiva, H.S. (2016). Simple approach to analyze the fully developed two-phase magneto convection type flows in inclined parallel-plate channels, Latin American Applied Research. 46: 93-98.
9. Sri Ramachandra Murty, P., Balaji Prakash, Karuna Sree, C. (2018). Rotating Hydro magnetic Two-Fluid Convective Flow and Temperature Distribution in an Inclined Channel. International Journal of Engineering and Technology. 7:4.10, 629-635.
10. Umavathi, J.C., Chamkha Ali, J., Manjula, M.H., and Al-Mudhaf, A. (2005). Flow and heat transfer of a couple stress fluid sandwiched between viscous fluid layers, Canadian Journal of Physics. 83: 705-720.

*Corresponding author.

11. Umavathi, J. C., Kumar, J.P., and Chamkha, A.J. (2008). Flow and heat transfer of a micro polar fluid sandwiched between viscous fluid layers. Canadian J. Phy. 86: 961-973.
12. Chauhan, D.S., and Rastogi, P. (2009). Hall current and heat transfer effects on MHD flow in a channel partially filled with a porous medium in a rotating system. Turkish Journal of Engineering and Environmental Sciences. 33: 3, 167-184. DOI: 10.3906/muh-0905-6.
13. Umavathi, J.C., Liu, I.C., Kumar, J.P., and Meera, D.S. (2010). Unsteady flow and heat transfer of porous media sandwiched between viscous fluids. Journal of applied Mathematics and Mechanics English edition. 31:12, 1497-1516.
14. Sheikholeslami, M., Ganji, D.D. (2014). Three dimensional heat and mass transfer in a rotating system using nanofluid. Powder Technology. 253: 789–796.
15. Sri Ramachandra Murty, P., and Balaji Prakash, (2016). Magneto hydrodynamic two-fluid flow and heat transfer in an inclined channel containing porous and fluid layers in a rotating system. Maejo International Journal of Science and Technology. 10:1, 25-40.
16. Karuna Sree, C., Sri Ramachandra Murty, P., and Sobhan Babu, K. (2020). Convective two-layered flow and temperature distribution through an inclined porous medium in a rotating system. Songklanakarin J. Sci. Technol. 42:2, 371-382.
17. Karuna Sree, C., Sri Ramachandra Murty, P., and Sobhan Babu, K. (2022). Convective flow and temperature distribution in rotating inclined composite porous and fluid layers. Songklanakarin J. Sci. Technol. 44:2, 370-380.
18. Rani, H.P., Leela, V., Nagabhushanam, P., and Gangadhar, R.R. (2021). Heat Transfer characteristics of Mixed Convective Magneto hydrodynamic Counter-Current Two-Phase Flow in Rotating Inclined Micro-Porous Channel with Slip Velocity and Asymmetric Thermal Boundary Conditions Using LTNE Model. J. Thermal Sci. Eng. Appl. 1-16
19. VeeraKumar, M., Ameer Ahmad, N., and Chamkha Ali, J. (2021). Numerical investigation on unsteady MHD convective rotating flow past an infinite vertical moving porous surface. In Shams Engineering Journal. 12:2, 2099-2109.

*Corresponding author.